

# Parameter estimation and deformation analysis of sand waves and mega ripples.

Roderik Lindenbergh

Mathematical Geodesy and Positioning, Delft University of Technology  
P.O. Box 5058, 2600 GB Delft, The Netherlands  
fax: +31 15 278 3711, mail: r.c.lindenbergh@geo.tudelft.nl

## Abstract

A time-series of interpolated multibeam data of non-parallel sand waves covered by mega ripples is analyzed on deformation. Parameters for a grid point wise, sinusoidal and time dependent model are identified, and estimated by a mixture of local and global statistical techniques.

## 1 Introduction.

It is very fascinating to find out that The Netherlands show much more relief under the sea than at land: sand waves with heights of around 10 meters and wavelengths of several hundreds of meters are covered by mega ripples that are about one tenth of the size of the sand waves. Moreover, both structures change on rather short time scales, [4].

These changes of sea bed topography are a possible cause of danger for passing ships. Therefore, parts of the North Sea are intensively monitored by Dutch authorities like the Royal Navy and the North Sea Directorate who have developed methods of predicting local sea bottom changes,[1, 9]. During the last fifteen years this monitoring has lead to an archive of singlebeam and multibeam echo data. In this article we analyze a time series of nine epochs of interpolated multibeam data covering a  $1\text{km}^2$  sand wave area near the main ship route from the Channel towards Rotterdam, see Figure 1.

We try to detect and quantify the deformation of the sand waves and, moreover, we identify and determine parameters that describe the movement of the mega ripples. Methods for detecting deformation out of data obtained by leveling were developed in the seventies at the geodesy department of Delft University of Technology, [7, 8] based on the Delft method of testing, [5, 6]. The data sets considered at that time were relatively small. The amount of data produced by modern survey equipment is much higher and asks for efficient, automatic methods. Still, the Delft method has already proved to be useful for deformation analysis of singlebeam, [1] and of laser altimetry data, [3]. In [3] models are tested for deformation at single grid positions. In [1] global models are considered as well, but it is assumed that the crest of the sand waves are parallel. This is clearly not the case in Figure 1. Therefore we will use a mixed local/global approach to estimate deformation parameters. In Sections 2 and 3 we identify these parameters and discuss the Delft method of deformation analysis, while in Section 4 we demonstrate how a first value for the identified parameters can be obtained. Finally, in section 5, we discuss the results and give directions for further research.

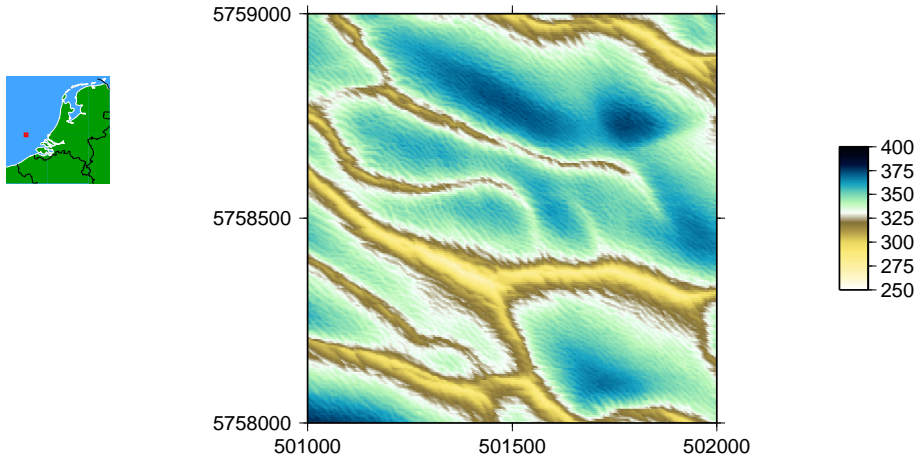


Figure 1: The considered part of the sea bottom in 2002. Depths are given in decimeters.

## 2 Expected deformation.

Before starting to model expected deformation, some feeling for the available data is required. Multibeam data interpolated to the same regular 5 meter grid is available for the years 1992 – 1997 and 2000 – 2002 covering an area of  $1\text{km}^2$ . This means that for every year approximately  $200 \times 200 = 40\,000$  heights are given. For every year the average, the minimal and the maximal depth are presented, in decimeters, in Table 1 (Columns 2, 3, and 4). Furthermore, the data from 1992 to 2001 were subtracted from the 2002 data. The results of this operation are listed in columns 5 to 8: here the average difference, the maximal upward difference and the maximal downward difference are presented. We conclude that the average difference is in the order of 1 dm, while differences up to a few meters may occur. The last column, NaN, reports the number of subtraction failures due to missing data.

year	$\bar{z}$	$z_{\min}$	$z_{\max}$	$\overline{\Delta z_{02}}$	max. dev.	min. dev	NaN
1992	338.2	268.6	380.5	1.48	43.4	-31.6	1282
1993	337.0	265.9	380.2	-0.38	32.0	-22.8	1139
1994	336.2	262.8	378.7	-0.29	30.0	-27.8	870
1995	338.5	272.3	379.0	1.47	29.6	-23.9	3330
1996	337.7	261.8	379.4	1.24	24.5	-23.0	864
1997	338.2	265.6	379.8	1.65	23.7	-21.4	874
2000	335.2	262.2	376.1	-1.35	24.0	-28.3	1231
2001	336.7	267.1	378.1	-0.21	23.0	-20.0	1905
2002	336.5	267.2	378.2				

Table 1: Some characteristics of the available data sets.

Analyzing Digital Elevation Models for every year gives the feeling that the bigger structures, the sand waves, are relatively stable. Only near position (501 415, 5 758 130) the narrow sand wave crest seems to connect to the bigger sand wave crest during the years. In Figure 1 the mega ripples are clearly visible, but the 2002 data seem of better quality than most of the other data.

A next step is to consider some difference plots. In Figure 2 the difference between the 1994 and the 2002

data is shown. Again, the mega ripples are clearly visible, which indicates that they are moving. Near the top of the crests, the differences seem to increase, while the deep areas seem relatively stable.

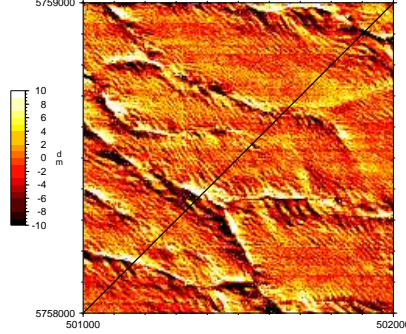


Figure 2: The difference between the 2002 and the 1994 data.

We conclude that at most positions the bigger features seem to be stable while the mega ripples are expected to move over the sea bottom.

### 3 Deformation modeling and testing.

We will concentrate on finding parameters for models describing deformation or motion at local scale, which means for us at grid point scale. If all data are available we have at every grid point an observation vector

$$\underline{y} = (h_{92}, \dots, h_{97}, h_{00}, h_{01}, h_{02})^T$$

of  $n = 9$  observations. When using a linear deformation model consisting of  $m$  parameters, we look for a parameter vector  $x \in \mathbb{R}^m$ , given a  $n \times m$  model matrix  $A$ . We model the error in the observation by a variance  $\sigma$ , while we assume that there is no correlation between different epochs. Therefore the covariance matrix  $Q_y$  is just a multiple of the identity matrix. The best estimation for the parameter vector is obtained by projecting the observation vector  $y$  into the model space, that is

$$\hat{x} = (A^T Q_y^{-1} A)^{-1} A^T Q_y^{-1} \underline{y}$$

By using the parameters found, we get adjusted observation parameters via  $\hat{y} = A\hat{x}$ . The weighted distance  $T_{n-m} = (y - \hat{y})^T Q_y^{-1} (y - \hat{y})$  is called the test statistic and gives an indication on the the quality of the approximation via the model  $A$ . The test statistic is compared to a critical value  $\kappa(\alpha, q)$  that depends on a level of insignificance  $\alpha$  and the degrees of freedom  $q = n - m$ . A linear model is said to be accepted if  $T(A) < \kappa_\alpha(A)$ . One can choose between different accepted models  $A_i$  by considering the quotient  $T/\kappa_\alpha$  for every model  $A_i$  and picking the model with the lowest test quotient as the most likely.

In the case that we consider, however, the simple linear models are not expected to be very adequate: due to the moving mega-ripples, the sea bottom is likely to be locally unstable, while it is unlikely that it will move up or down at constant speed. Therefore it was not a surprise that the  $m = 1$  linear model that models a locally stable sea bottom of height  $h$ , and the  $m = 2$  linear model that tests for positions that move up or down from initial position  $h$  with constant speed  $v$ , gave only little positive response. Positions that test

positively are situated in the deeper parts. This confirms that the mega ripples have smaller amplitudes when located off the sand wave crests.

The results of the tests described above caused us to consider a more complicated deformation model. To give a local description of the motion of the mega ripples we use the equation that describes a plane wave that is propagating in one direction:

$$\psi(x, y, A, k, \phi_0, \theta, v, t) := A \sin[k(x \cos \theta + y \sin \theta) - vt + \phi_0] \quad (1)$$

Here  $A$  denotes the amplitude of the wave,  $k$  the wave number,  $\phi_0$  the initial phase,  $\theta$  the angle between the propagation direction of the wave and the horizontal  $x$ -axis, while  $t$  stands for time and  $v$  for wave velocity. An example of such wave with  $\theta = \pi/6$  and  $v = 0$  is shown in Figure 3.

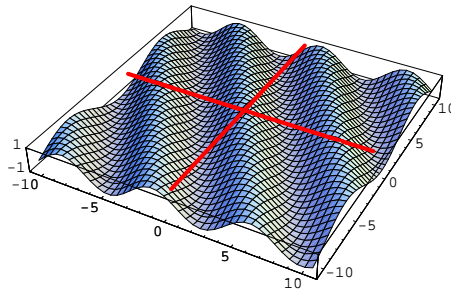


Figure 3: A plane wave with parameters  $A = k = 1$ ,  $\phi_0 = \pi/2$  and  $\theta = \pi/6$ .

It is not clear how to write Equation 1 in such a way that the parameters are in linear relation with the depth values in the different years. Moreover, the number of parameters initially unknown ( $A, k, \phi_0, \theta, v$ ) is high compared to the number of data available per grid point location (at most 9). Therefore it is not feasible to determine the parameters per grid point. Instead we will discuss methods in the next section on finding good parameter values at more global scales. In the end, once all parameters values are fixed, one can come back to Equation 1 and use the grid point data to evaluate the wave function with the parameters found. Again, by analyzing the weighted distance between the observation vector and the wave model one can, on one hand, get insight in the fit of the observations in the model and, on the other hand, determine how well the model fits compared to other models, like the linear models discussed above.

## 4 Determining parameters for the local wave function.

In this section we discuss different methods that work on different scales for determining the parameters of the wave function as identified above.

### Global wavenumber.

The first parameter that we consider is the wave number  $k$ , or equivalently, the wavelength  $\lambda = 2\pi/k$ . We assume that the wavelength is more or less constant over the years. Therefore we use the good quality 2002 data to determine it. We assume for the moment that the wavelength is independent of the location as well. If this assumption is justified we can determine it by a simple counting procedure. For this purpose we use the difference of the original 2002 data and a smoothed version of the data, obtained by a nearest neighbour

interpolation implemented in GMT with suitable parameters. On the resulting difference plot, the mega ripples are clearly visible. As most ripples seem to run from the South-West to the North-East, we count the number of mega ripple crests along the SW-NE diagonal, that has a length of 1414 meter. We find 90 crests, which corresponds to a wavelength of approximately 16 meter.

### Local wave direction.

When looking at Figure 1, one gets the impression that the direction of the mega ripples is more or less parallel to the direction of the sand waves. As the sand waves are not really parallel themselves this implies that there is a local variation in the mega ripple direction. The sand waves are more or less constant over the years, therefore we once again use the 2002 data to estimate the local wave direction.

First we shortly discuss a method that did not work. In order to determine the wave direction  $\theta_{(x,y)}$  at grid point  $(x, y)$  we used differently sized blocks of surrounding grid points. We determined the best fitting plane wave of the form  $\psi = A \sin[k(x \cos \theta + y \sin \theta) + \phi_0]$  with parameters as in Equation 1, and  $k$  as determined above. Unfortunately the results were neither much spatially correlated nor showing connection with Figure 1. Most probably the available data are too sparse.



Figure 4: Low variation in the red strips, high variation in the blue strips.

An alternative method did work out however. This method consists of determining variation in different discrete directions for a block of measurements. The direction with the lowest variation is in theory almost parallel to the crests of the mega ripples as present in the block.

We define and determine the variation in direction  $\theta$  for at most  $n \times n$  regular  $xyz$  data positioned in a block by the following procedure.

1. Let

$$R_\theta = \begin{pmatrix} \cos \theta & \sin \theta \\ -\sin \theta & \cos \theta \end{pmatrix}$$

be the *rotation matrix* that rotates vectors over an angle  $\theta$  around the origin  $(0, 0)$ .

2. Rotate all  $(x, y)$  values in the block. Determine the minimal  $y_-$  and maximal  $y_+$  value *after* rotation. Define the strip width  $w_\theta := (y_+ - y_-)/n$ . Divide the height  $z$  of an grid triple  $(x, y, z)$  into horizontal strips according to their rotated  $y$ -value, that is, according to  $R_\theta(y)$ :

$$[y_-, y_- + w_\theta), \dots, [y_- + (m - 1) \cdot w_\theta, y_- + m \cdot w_\theta)$$

such that  $y_- + (m - 1) \cdot w_\theta \leq y_+ < y_- + m \cdot w_\theta$ . As a consequence, every grid height belongs now to exactly one strip.

3. Suppose that  $z_i$  belongs to strip  $S_k$ . Then the *individual variation* of  $z_i$  is defined as  $v_\theta(z_i) = z_i - \mu_k$  where  $\mu_k$  denotes the average height of the heights in strip  $S_k$ .
4. The *overall variation* in direction  $\theta$  is just the sum of squares of all individual variations:  $V_\theta = \sum_i v_\theta(z_i)^2$ .

As an example we consider Figure 4, on the left. In the direction  $\theta = 0$ , the heights are divided into the red strips, so all individual variations equal 0, as does the overall variation:  $V_0 = 0$ . In the direction  $\theta = \pi/4$  however, the individual variations vary, as the height values per strip vary, see Figure 4, on the right, where the individual variations are shown. In this case, the overall variation is given by  $V_{\pi/4} = 5/3$ .

For a block of grid data that contains a maximum of  $n \times n$  heights (Some heights are missing due to e.g. measurement errors), we consider the  $2n$  directions

$$-\pi/2, -\pi/2 + \pi/(2n), \dots, \pi/2 - \pi/(2n).$$

For every direction we compute the overall variation and we pick the direction that has minimal variation as an approximation of the local mega ripple crest direction. This is demonstrated in Figure 5, where blocks of  $40 \times 40$  meter are analyzed. In the middle of every block the direction computed with the method just described, is indicated by a short red line. Note that the mega ripples pass the crests of the sand waves in the direction perpendicular to the direction of the crest. It is also clear that the directions as computed show correlation with neighbouring directions.

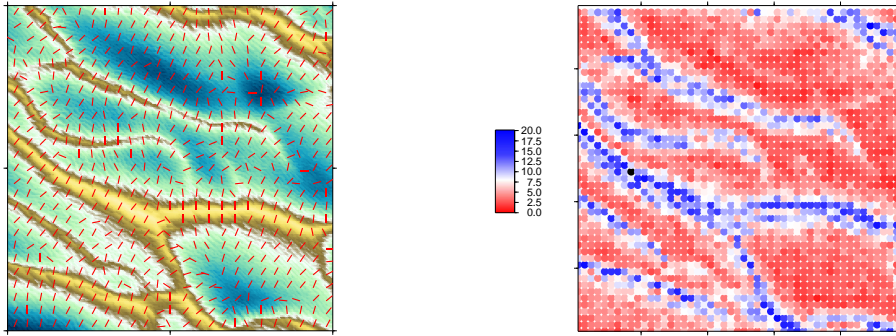


Figure 5: The local direction of the mega ripples indicated by the red lines, on the left. On the right, the amplitude of the mega ripples in decimeters.

### Local amplitude.

Figure 2 suggests that the amplitude of the mega ripples varies with the depth of the sand waves. We verify this by considering  $20m \times 20m$  blocks for the 2002 data. If all grid points are available, such blocks contain 16 heights. If 15 random heights of the sine function are determined, the difference between the maximum height and the minimum height presents is on average near to 1.93. Therefore we multiply the difference between the maximal and minimal height per block by  $1/1.93/2 = 0.518$  to get a first estimate of the mega ripple amplitude, as a function of the position. The result, that clearly demonstrates the relation between the amplitude of the mega ripples and the position of the ripples on the sand waves, is shown on the right in Figure 5.

## Global speed.

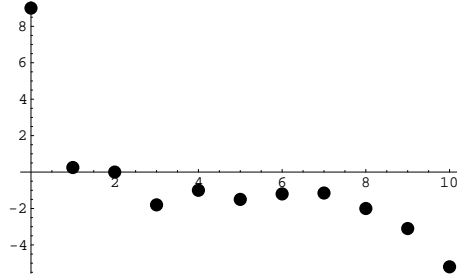


Figure 6: Covariogram of variation of height in times at all grid points shows periodic correlation.

The final parameter that is left, is the propagation velocity  $v$  of the mega ripples. We assume that this parameter is independent of the position of the mega ripples in the sand wave landscape and, moreover, we assume that the velocity is constant over the years. This implies that we can use all data of all years available to determine the velocity. For a first guess we assume that the data in all years was obtained at the same moment, which means that we can represent the echo acquisition data by  $t = 1, 2, 3, 4, 5, 6, 9, 10, 11$ . In this way we obtain for each position a set of height data such that, by assumption, each data point should demonstrate the same periodic behaviour. As in [1], we trace the periodicity by means of the *covariogram* of the data, see also [2]. For each grid point  $i$ , we determine the average height  $\bar{z}_i$  over the years and the differences  $dz_{ji} = z_{ji} - \bar{z}_i$  between the individual height  $z_{ji}$  in year  $j$  and the average height. In a next step we collect all such differences at all grid points for any time interval between two loading data. This results in an empiric covariance function, see Figure 6. This covariance function demonstrates periodicity, but smaller time intervals are needed to conclude that the period that shows up in the covariogram is indeed only one period in the propagation of the mega ripples.

## 5 Further Research and Conclusions.

In this article we have shown how to obtain parameters for more complicated deformation models by exploiting time series of  $xyz$  data on different spatial and temporal scales. A next step is to substitute the parameters found into the wave function in order to get insights in the quality of the model and the parameter values. Better parameter values can be obtained by considering the data in more detail, for example, the mega ripple velocity should be computed by considering the exact months of acquisition, rather than the years of acquisition. For this article, we have analyzed interpolated multi beam data. The original data contain much more detail, but when analyzing these data more attention should be given to the computational efficiency. Also alternatives for the wave model should be considered.

## Acknowledgements.

The author wishes to thank Ben Diericx and Simon Bicknese from the North Sea Directorate for providing him with the data and for their useful remarks. From TNO-FEL, Dick Simons and from the DEOS department, Ramon Hanssen, Gini Ketelaar, Hans van der Marel, Norbert Pfeifer and Mirjam Snellen are thanked for useful comments and help with the pictures.

## References

- [1] L.L. Dorst. Zeebodemmonitoring met geostatistiek en deformatieanalyse. Technical report, Koninklijke Marine, Dienst der Hydrografie, 2003.
- [2] E. I. Isaaks and R. M. Srivastava. *Applied Geostatistics*. Oxford University Press, 1989.
- [3] Roderik Lindenbergh and Ramon Hanssen. Eolian deformation detection and modeling using airborne laser altimetry. In *2003 IEEE International Geoscience and Remote Sensing Symposium*, pages 1–4, Toulouse, France, 2003. CDROM.
- [4] Attila A. Nemeth. *Modelling offshore sand waves*. PhD thesis, Universiteit Twente, 2003.
- [5] P. J. G. Teunissen. *Adjustment theory; an introduction*. Delft University Press, Delft, 2000.
- [6] P. J. G. Teunissen. *Testing theory; an introduction*. Delft University Press, Delft, 2000.
- [7] J. van Mierlo. A testing procedure for analysing geodetic deformation measurements. In *Proceedings, Second International Symposium on Deformation Measurements by Geodetic Methods*, pages 321–353, Bonn, Germany, 1978.
- [8] H. M. E. Verhoef. Geodetische deformatie analyse, 1997. Lecture notes, Delft University of Technology, Faculty of Geodetic Engineering, in Dutch.
- [9] J.C. Wüst. Data-driven probabilistic predictions of bathymetry. In *Proceedings of International Workshop on Marine Sand Wave and River Dune Dynamics II, 2004*, Twenthe, The Netherlands, To appear.